QUASIELASTIC NEUTRINO SCATTERING*

R. L. Kustom, D. E. Lundquist, T. B. Novey, and A. Yokosawa

Argonne National Laboratory, Argonne, Illinois 60439

and

Frank Chilton

Stanford Research Institute, Menlo Park, California 94025

(Received 15 January 1969)

Quasielastic scattering of neutrinos, $\nu + n \to p^+ + \mu^-$, was measured in a 30-ton spark-chamber detector. Analysis of the cross section versus momentum transfer yields a value of $M_{A_1} = 0.7 \pm 0.15$ for a single-pole–type axial-vector form factor or $M_{A_2} = 1.05 \pm 0.2$ for a double-pole form factor. No decrease in cross section at low momentum transfer expected due to nuclear effects was observed.

We have studied the quasielastic scattering of neutrinos in the reaction $\nu + n \to p^+ + \mu^-$ in a neutrino beam prepared in the external proton beam of the Argonne Zero-Gradient Synchrotron (ZGS). The detector was a 30-ton assembly of steel plates and spark chambers previously described.[1-3]

Top and side views of the apparatus are shown in Fig. 1. The neutrino beam is prepared via the ZGS fast extraction system.[4] 50% of the circulating proton beam was extracted in about 50 μsec. A beryllium target, 3 cm in diameter and 60 cm long, was located in a current-sheet focusing horn[5] pulsed to a current of 150 kA. The horn is followed by a 50-ft drift space for pion decay and a shielding layer of concrete and steel sufficient to stop muons up to 16 BeV. The detector, 6 ft square and 12 ft long, was enclosed in a steel shield room with 12-in. wall and ceiling thicknesses in turn surrounded by an anticoincidence

shield 8 ft high, 20 ft wide, and 16 ft long, which enclosed the detector and its optical system.

The neutrino flux at the detector was computed using several independently developed computer programs.[6] These programs take into account the focusing of the horn as well as the probability for neutrinos reaching the detector from decays in various parts of the drift space. Measurements of the pion focusing properties of the horn have been reported.[5] The intensity of protons hitting the target was measured by polyethylene and aluminum-foil activation and also by a secondary-emission detector.[7] These monitors determine the proton intensity to approximately 5%.

The original measurements[8] of the spectrum of angle and momentum for π^+ production have been used to compute the shape of the neutrino spectrum from the beryllium target; however, more recent measurements by Marmer et al.,[9] Asbury et al.,[10] and Marmer and Lundquist[11] are in disagreement with the original survey.

For this experiment we have computed the values of the ratios of positive-pion fluxes in the original survey to the more recent measurements[9,11] at 3° at 1.0, 1.5, 2.0, and 2.5 GeV/c. Using these ratios to reweigh the 0.4-, 0.6-, 0.8-, and 1.0-GeV/c neutrino flux gives an average overall increase in the neutrino flux of 1.5. This inexact procedure based on incomplete data does not allow us to claim knowledge of the absolute flux to better than ±30%. Final determination of the neutrino flux must await new measurements of the π^+ production cross section from beryllium.

Figure 2(a) shows the corrected neutrino spectrum.

The detector consisted of 66 $\frac{1}{2}$-in.-thick steel plates, 66 two-gap spark chambers, and 22 plastic scintillator sheets.[3] The spark chambers
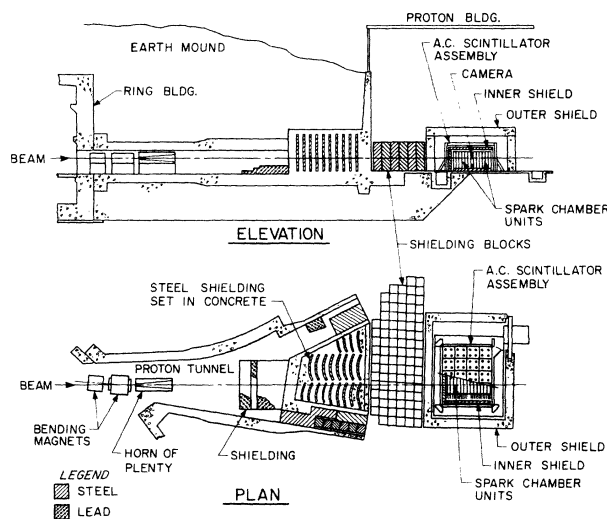

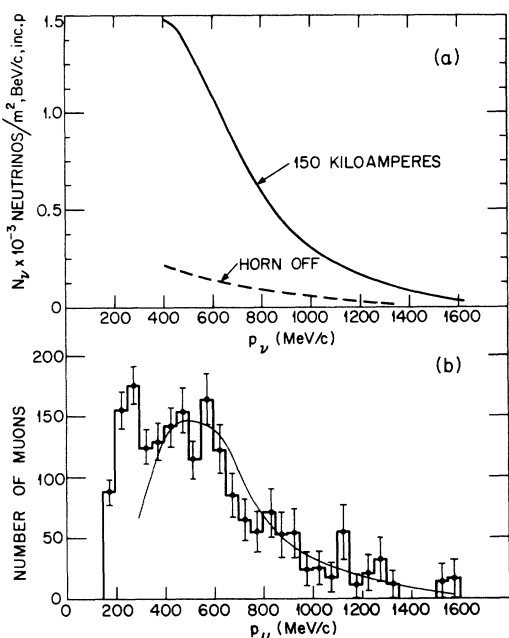FIG. 1. Top and side views of the ZGS neutrino experiment.

FIG. 2. (a) Neutrino spectrum with the horn at 0 and 150 kA. (b) Muon spectrum, observed elastic events. The solid curve is calculated from the theoretical cross section and the neutrino-spectrum shape.

were photographed via a series of 66 mirrors, one for each spark chamber producing a cylindrical Fresnel lens. In addition to the stereo spark-chamber cameras, a third camera recorded from a four-trace oscilloscope display the rf structure of the beam, the presence of any pulse from the cosmic-ray anticoincidence shield, and any signals from each of the scintillator sheets in the detector. The trigger signal for the spark chamber electronics was the presence of a pulse in any two sequential scintillator sheets during a gated on time of 100 μsec. This requires a minimum particle range of 40 g/cm^2. The rate of triggering primarily due to accidental cosmic-ray events is about 1 in every 15 machine pulses. The rate of neutrino triggers was approximately 1 in every 200 pulses.

The anticoincidence shield signals were recorded but were not used to veto electronically the system trigger. This would have eliminated a set of neutrino events where one track left the detector and penetrated the steel shield room. We recorded all neutrino events along with accidental cosmic-ray tracks during the beam spill and eliminated the background using the recorded veto signal during the film scanning.

During the four one-week runs, the machine intensity average 10^{12} protons/pulse and a total of

3×10^{17} protons were extracted onto the target. The total neutrino trigger rate was approximately 200 events/day for a total of 6000 neutrino triggers. Half these triggers were due to events originating outside the detector volume.

The film was double scanned to select events with vertices inside the detector fiducial volume with 95% efficiency. The events observed were 80% single track, 15% two prong, and 5% >two prong or with showers present. The distribution of events throughout the detector volume was uniform as expected for weakly interacting neutral particles. The fiducial volume limits were 2 in. from the chamber edges. No edge effects were observed. The number of scattering (>10°) of the single-prong events gives a limit of less than 3% strongly interacting particle content. Hence, the tracks were taken to be muons.

Accepted for the "elastic" sample were all single-track stopping events and all two-prong stopping events which could fit an elastic event allowing generously for the range of Fermi motion. This sample contained 90% single tracks and 10% two-prong events. There was also an additional criteria of a minimum muon momentum of 300 MeV. This allowed additional discrimination against inelastic events as well as limiting the events to the region in which the neutrino spectrum was known.

In order to correct these events to the total production rate, an average stopping probability for muons of various direction and momenta inside the detector was computed. Each event was then assigned a statistical weight corresponding to the inverse of the stopping probability.

We have used the cross-section ratios and inelastic cross-section shapes given by Berman and Veltman[12] to predict a total inelastic contribution of 30% for the ZGS neutrino spectrum. The inelastic channel via N_{1236}^* or higher resonances results in a shift of the muon momentum to lower values. With the 300-MeV/c minimum momentum cutoff and the elimination of obvious multiprong inelastic events there remains a background from this calculation of 10 ± 5% inelastic events in the "elastic" sample. This correction was made as 10% proportional subtraction.

We have alternatively attempted to estimate the number of muons >300 MeV/c associated with N^* production using measurements from the 1964-1965 Freon (CF$_3$Br) bubble-chamber experiments at CERN.[13] In Fig. 2(b), the background of muons from N^* production would be expected to rise for successively lower values of p_μ down to 300

MeV/c. Events with p_μ of 300 to 400 MeV/c fall predominantly into the low–momentum-transfer bins, $t < 0.1$ (BeV/$c)^2$, on the distributions shown in Figs. 3(b) and 3(c). This estimate would give an upper limit of 20 to 25% inelastic events rather than 10%.
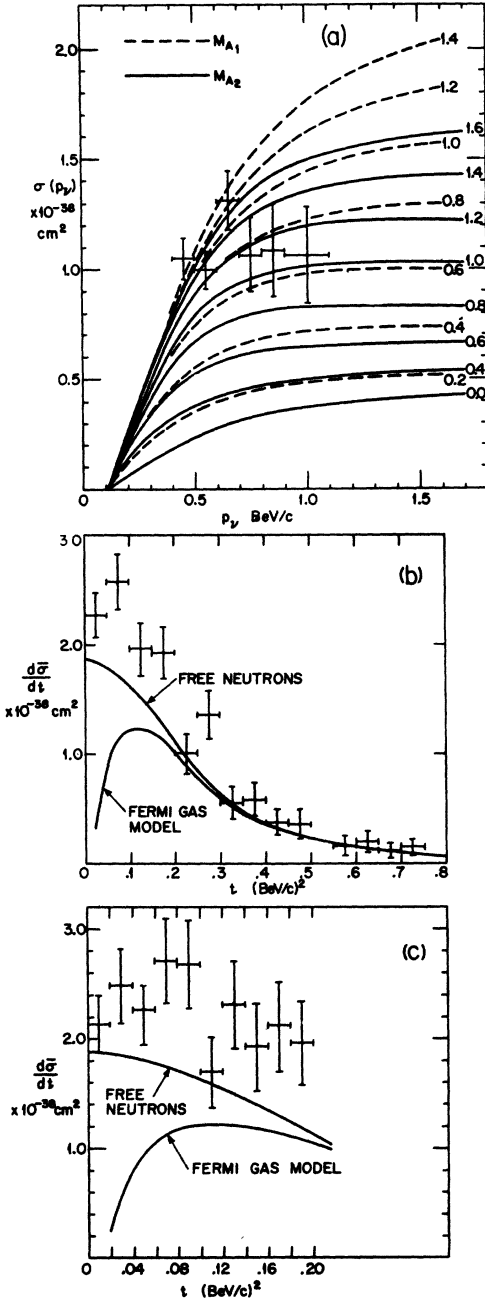

FIG. 3. (a) Measured neutrino elastic cross sections and calculated cross sections for two types of axial-vector form factors. (b) Comparison of observed $d\sigma/dt$ with cross sections predicted on free neutrons and neutrons in a Fermi-gas distribution, $P_F = 270$ MeV/c. (c) Same as (b) with expanded t scale.

The difference in our two estimates arises principally from the shapes of the rise of the inelastic total cross section with neutrino energy in the region of threshold to 1.0 GeV, as given in Refs. 12 and 13.

Figure 2(b) shows a plot of the weighted observed muon spectrum in all single-track stopping events. The curve is the calculated elastic muon spectrum for a typical form factor, $MA_1 = 0.8$ GeV. Inclusion of nuclear effects has little effect on this spectrum shape which principally reflects the neutrino spectrum shape in this forward angular region. The calculated muon spectrum from elastic interactions fits the observed data above 300 MeV/c. The excess of low-energy muons below 300 MeV is presumably associated with N^* production.

The incident neutrino energy can be calculated for each event from the muon momentum vector if the target neutron is at rest:

$$P_\nu = \frac{E_\mu - m_\mu^2/2m_p}{1 - m_p^{-1}(E_\mu - p_\mu \cos\theta_{\mu\nu})}.$$

This expression can be used with less than 10% error for the case where Fermi motion is present for muons produced at forward angles $\theta_\mu < 70°$. The event rate combined with the neutrino spectrum gives $\sigma(p_\nu)$ shown in Fig. 3(a). The solid curves are calculated using a double-pole axial-vector form factor and the dotted curves are for a single-pole case described in Eq. (3) below.

For interaction with a nucleon at rest the momentum transfer

$$t = -q^2 = \frac{m_\mu^2 - 2E_\mu(E_\mu - p_\mu \cos\theta_{\mu\nu})}{1 - m_p^{-1}(E_\mu - p_\mu \cos\theta_{\mu\nu})}. \qquad (1)$$

We calculate the "effective momentum transfer" for our events, t_{eff}, using Eq. (1) and compare this distribution with theory[14] by folding in the ZGS neutrino spectrum and desired nuclear model.

The nuclear momentum distribution in the nucleus has little effect on the momentum-transfer calculation in this forward production region.[1]

The number of events predicted are related to the cross section by

$$\frac{dN}{dt} = N_p N_T \int \frac{d\sigma}{dt} N(p_\nu)dp_\nu = N_p N_T N_\nu \frac{d\sigma}{dt},$$

where N_p is the number of beam protons (3×10^{17}),

N_T is the number of target neutrons per cm^2 in the detector fiducial volume (2.7×10^{26}), and N_ν is the average number of neutrinos passing through the fiducial volume per incident-beam proton onto the horn target (2.4×10^{-3}).

The observed cross sections per neutron in the detector fiducial volume are shown in Fig. 3(b). The errors are computed from event statistics and do not include the uncertainty in neutrino flux. Figure 3(c) shows the data in the small momentum-transfer region, $0 < t < 0.2$ (BeV/c)^2. The solid lines on Figs. 3(b) and 3(c) are the theoretical cross sections for a free-neutron target and for bound neutrons in the Fermi-gas approximation ($P_F = 270$ MeV/c).

The shape indicated by the experimental data is close to that of the free-neutron cross section. A χ^2 fit of this data to the free-neutron cross section using vector form factors of the form

$$ G_E(t) = \frac{1}{4.71} G_m(t) = \left(\frac{1}{1 - t/M_\nu^2} \right)^2, \qquad (2) $$

and taking the value[15] $M_\nu^2 = 0.71$ and an axial-vector form factor

$$ F_{A_n} = \left(\frac{1}{1 - t/M_{A_n}^2} \right)^n, \quad n = 1 \text{ or } 2 \qquad (3) $$

yields $M_{A_1} = 0.7 \pm 0.15$ BeV and $M_{A_2} = 1.05 \pm 0.2$ BeV.

These two choices for one-parameter form factors give two different shapes and asymptotic behaviors for interpretation of experiment. Roughly, $M_{A_2} \sim \sqrt{2} M_{A_1}$ provided the fit is to data with $t < M_A^2$.

The absence of large nuclear effects at energy transfer comparable and smaller than nuclear binding energies was unexpected.[16,17]

We would need a more detailed knowledge of the inelastic cross sections below neutrino energy of 1 GeV to interpret this result.

*Based on work performed under the auspices of the U. S. Atomic Energy Commission.

[1]T. B. Novey, Proc. Roy. Soc. (London), Ser. A 301, 113 (1967).

[2]V. L. Telegdi, Brookhaven National Laboratory Report No. BNL 837 C39, 1963 (unpublished), p. 170.

[3]T. B. Novey, CERN Report No. CERN 65-32, 1965 (unpublished), p. 31.

[4]S. Suwa and A. Yokosawa, Nucl. Instr. Methods 52, 277 (1967).

[5]H. Vogel, W. Brunk, E. Roberts, F. Markley, I. Pollack, H. Hintenberger, V. L. Telegdi, and R. Winston, in Proceedings of the International Symposium on Magnet Technology, Stanford Linear Accelerator Center, Stanford, Calif. (unpublished), pp. 650-656.

[6]A. Aesner and Ch. Iselin, CERN Report No. CERN 65-17 (unpublished); D. D. Jovanovic, L. R. Thebaud, and C. Smith, private communication; R. Winston, private communication; Y. Cho, private communication.

[7]A. F. Stehney and E. P. Steinberg, Nucl. Phys. B5, 188 (1968).

[8]R. A. Lundy, T. B. Novey, D. D. Yovanovitch, and V. L. Telegdi, Phys. Rev. Letters 14, 504 (1965).

[9]G. J. Marmer, K. Reibel, D. M. Schwartz, A. Stevens, T. A. Romanowski, C. J. Rush, P. R. Phillips, E. C. Swallow, R. Winston, and D. Wolf, Argonne National Laboratory Report No. HEP 6801 (unpublished).

[10]J. G. Asbury, Y. Cho, M. Derrick, L. G. Ratner, T. P. Wangler, A. D. Krisch, and M. T. Lin, Argonne National Laboratory Report No. ANL/HEP 6820 (unpublished).

[11]G. J. Marmer and D. E. Lundquist, private communication.

[12]S. Berman and M. Veltman, Nuovo Cimento 38, 993 (1965).

[13]E. C. M. Young, CERN Report No. CERN 67112, 1967 (unpublished).

[14]T. D. Lee and C. N. Yang, Phys. Rev. 126, 2239 (1962); F. Chilton, Nuovo Cimento 31, 447 (1964); J. Loevseth, Phys. Letters 5, 199 (1963).

[15]See, e.g., G. Weber, in Proceedings of the Third International Symposium on Electron and Photon Interactions at High Energies, Stanford Linear Accelerator Center, 1967 (Clearing House of Federal Scientific Technical Information, Washington, D. C., 1968), p. 59.

[16]V. L. Telegdi, private communications; S. Berman, CERN Report No. CERN 61-22 (unpublished); B. Goulard and H. Primakoff, Phys. Rev. 135, B1139 (1964).

[17]C. W. Kim and M. Ram, Phys. Rev. Letters 20, 35 (1968).